

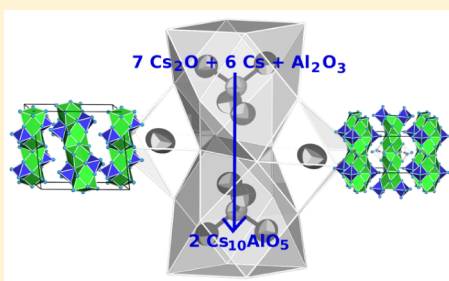
## Alkali Metal Suboxometalates—Structural Chemistry between Salts and Metals

Matthias Wörsching and Constantin Hoch\*

Department Chemie, Ludwig-Maximilians-Universität München, Butenandtstraße 5–13, D-81377 München, Germany

Supporting Information

**ABSTRACT:** The crystal structures of the new cesium-poor alkali metal suboxometalates  $\text{Cs}_{10}\text{MO}_5$  ( $\text{M} = \text{Al}, \text{Ga}, \text{Fe}$ ) show both metallic and ionic bonding following the formal description  $(\text{Cs}^+)_7(\text{MO}_4^{5-})(\text{O}^{2-}) \cdot 3\text{e}^-$ . Comparable to the cesium-rich suboxometalates  $\text{Cs}_9\text{MO}_4$  ( $\text{M} = \text{Al}, \text{Ga}, \text{In}, \text{Fe}, \text{Sc}$ ) with ionic subdivision  $(\text{Cs}^+)_9(\text{MO}_4^{5-}) \cdot 4\text{e}^-$ , they contain an oxometalate anion  $[\text{M}^{\text{III}}\text{O}_4]^{5-}$  embedded in a metallic matrix of cesium atoms. Columnlike building units form with prevalent ionic bonding inside and metallic bonding on the outer surface. In the cesium-rich suboxometalates  $\text{Cs}_9\text{MO}_4$ , additional cesium atoms with no contact to any anion are inserted between columns of the formal composition  $[\text{Cs}_8\text{MO}_4]$ . In the cesium-poor suboxometalates  $\text{Cs}_{10}\text{MO}_5$ , the same columns are extended by face-sharing  $[\text{Cs}_6\text{O}]$  units, and no additional cesium atoms are present. The terms “cesium-rich” and “cesium-poor” here refer to the  $\text{Cs}: \text{O}$  ratio. The new suboxometalates  $\text{Cs}_{10}\text{MO}_5$  crystallize in two modifications with new structure types. The orthorhombic modification adopts a structure with four formula units per unit cell in space group  $Pnnm$  with  $a = 11.158(3)$  Å,  $b = 23.693(15)$  Å, and  $c = 12.229(3)$  Å for  $\text{Cs}_{10}\text{AlO}_5$ . The monoclinic modification crystallizes with eight formula units per unit cell in space group  $C2/c$  with  $a = 21.195(3)$  Å,  $b = 12.480(1)$  Å,  $c = 24.120(4)$  Å, and  $\beta = 98.06(1)^\circ$  for  $\text{Cs}_{10}\text{AlO}_5$ . Limits to phase formation are given by the restriction that the M atoms must be trivalent and by geometric size restrictions for the insertion of  $[\text{Cs}_6\text{O}]$  blocks in  $\text{Cs}_{10}\text{MO}_5$ . All of the suboxometalate structures show similar structural details and form mixed crystal series with statistical occupation for the M elements following the patterns  $\text{Cs}_9(\text{M}^1_x\text{M}^2_{1-x})\text{O}_4$  and  $\text{Cs}_{10}(\text{M}^1_x\text{M}^2_{1-x})\text{O}_5$ . The suboxometalates are a new example of ordered intergrowth of ionic and metallic structure elements, allowing for the combination of properties related to both ionic and metallic materials.



### INTRODUCTION

In intermetallic compounds from metals with a high electronegativity difference, the metallic bond gets polarized. The extreme case is known as Zintl compounds, where the electron transfer can be assumed to be complete, resulting in ion formation. Less polar metal–metal bonding normally results in overall metallic behavior, but with high specific resistivity and nonlinear temperature dependence, sometimes described by the term “bad metal behavior”.<sup>1</sup> This kind of polar metallic bonding has interesting consequences for both properties and crystal structures.

Model substances for the study of polar metal–metal bonding can principally be accessed by two different synthetic routes. First, two metallic educts with a considerable electronegativity difference can react to form a product with more or less electron transfer from the electropositive to the electronegative partner.<sup>2</sup> Second, an ionic educt and a metallic educt can react to form a product still containing both basic bonding situations. This second synthetic strategy can lead to interesting crystal structures and a combination of the properties of both salts and metals. The cesium suboxometalates we present here are excellent examples of products of this second approach.

In 2009 we reported the preparation, structures, and properties of the cesium suboxometalates  $\text{Cs}_9\text{MO}_4$  ( $\text{M} = \text{Al}, \text{Ga}, \text{Fe}, \text{Sc}, \text{In}$ ).<sup>3</sup> They were obtained from reactions of the oxides, i.e.,  $\text{M}_2\text{O}_3$  and  $\text{Cs}_2\text{O}$ , with metallic cesium at temperatures of about 300 °C. As all of the suboxometalates  $\text{Cs}_9\text{MO}_4$  crystallize isotropically, mixed crystal series with different trivalent metals M can be prepared.<sup>3</sup> In their crystal structures, compartments with ionic bonding and compartments with metallic bonding alternate in an ordered pattern. This structural motif has previously been described extensively for alkali metal suboxides and alkaline-earth metal subnitrides.<sup>4,5</sup> In those compounds, the anionic part is constituted from monatomic oxide ( $\text{O}^{2-}$ ) or nitride ( $\text{N}^{3-}$ ) anions, whereas in the suboxometalates the anionic part is built from complex oxometalate anions  $[\text{M}^{\text{III}}\text{O}_4]^{5-}$ . This leads to a higher variety of possible anions by alternation of M.

The alkali metal suboxides and the alkaline-earth metal subnitrides are built from discrete cluster entities. The structures of rubidium suboxides are based on dimers of face-sharing oxide-centered octahedra  $[\text{Rb}_2\text{O}_2]$  and those of cesium suboxides on trimers  $[\text{Cs}_3\text{O}_3]$ . These clusters are closely packed in the crystal structures of  $\text{Rb}_9\text{O}_2$  and  $\text{Cs}_{11}\text{O}_3$ . In suboxides with higher metal content, a number of additional metallic alkali metal atoms are intercalated. Akin to the alkali metal suboxides, the crystal

Received: May 14, 2015

Published: July 1, 2015

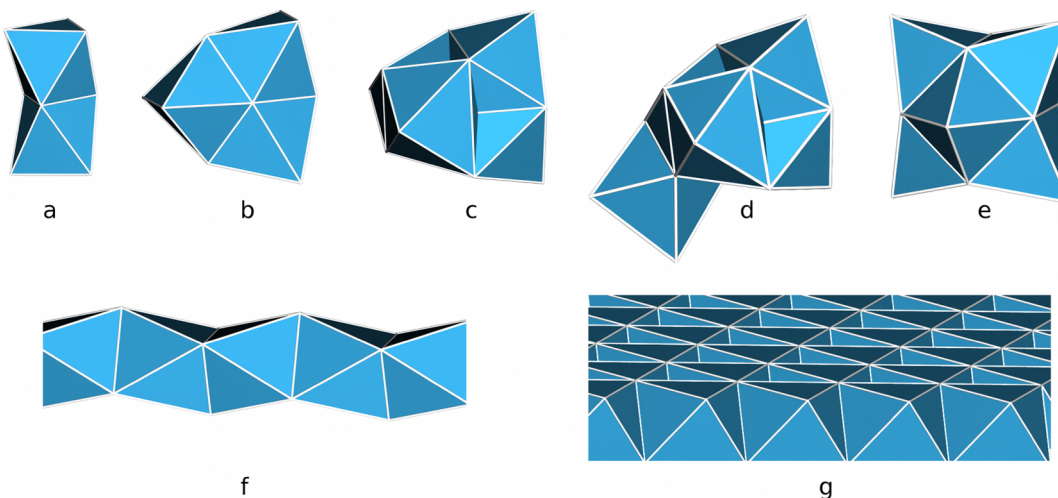


**Figure 1.** Clusters as structural building units in suboxides, subnitrides, and suboxometalates based on connected octahedra: (a) two octahedra in  $\text{Rb}_9\text{O}_2$ ; (b) three octahedra in  $\text{Cs}_{11}\text{O}_3$ ; (c) four octahedra in  $\text{Cs}_9\text{MO}_4$ ; (d) five octahedra in  $\text{Cs}_{10}\text{MO}_5$ ; (e) six octahedra in  $\text{Na}_{14}\text{Ba}_{14}\text{CaN}_6$ ; (f) infinite chain of octahedra in  $\text{Ba}_3\text{N}$  and  $\text{Cs}_3\text{O}$ ; (g) infinite sheet of octahedra in  $\text{Cs}_2\text{O}$ .

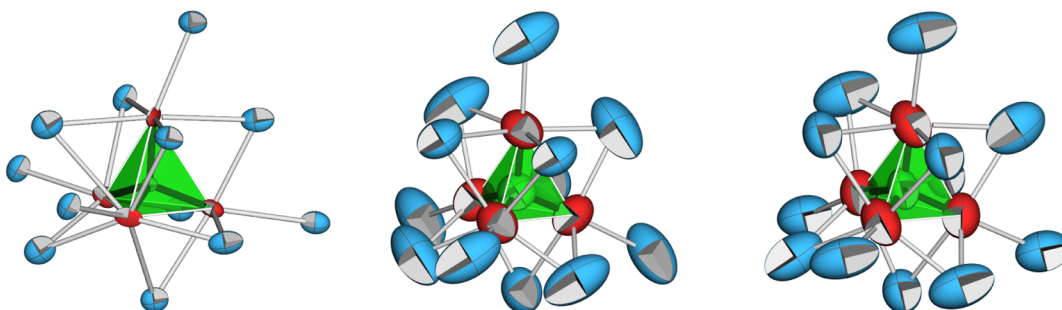


**Figure 2.** Juxtaposition of the  $[\text{GaO}_4]^{5-}$  oxometalate anions in (left)  $\text{Rb}_5\text{GaO}_4$ , (center)  $\text{Cs}_8\text{GaO}_4$ , and (right)  $\text{Cs}_{10}\text{GaO}_5$ , together with their respective coordination by alkali metal cations. The topological analogy is evident. Blue spheres, alkali metal atoms; red spheres, oxygen atoms; green spheres, gallium atoms; green tetrahedra,  $[\text{GaO}_4]^{5-}$  anions. All ellipsoids are drawn at a probability level of 90%.

structure common to all of the cesium suboxometalates  $\text{Cs}_9\text{MO}_4$  is built from polyhedral cluster entities. Where the small oxide (or nitride) anions in alkali metal suboxides (or alkaline-earth metal subnitrides) are coordinated octahedrally by cesium (or barium), the bigger tetrahedral oxometalate anions  $[\text{MO}_4]^{5-}$  in the cesium suboxometalates are coordinated by 12 cesium atoms in a distorted cuboctahedron  $[\text{Cs}_{12}\text{MO}_4]$ . This cuboctahedron is the result of the octahedral coordination of each of the four oxygen atoms of the  $[\text{MO}_4]^{5-}$  anion by five cesium atoms and one M atom. The  $[\text{Cs}_{12}\text{MO}_4]$  cuboctahedra are condensed by sharing of common faces to form  $^1_{\infty}[\text{Cs}_8\text{MO}_4]$  columns as building blocks corresponding to the cluster entities in suboxides and subnitrides. Metallic cesium atoms are intercalated between these columns, creating the metallic substructure. A compilation of building units in suboxides, subnitrides, and suboxometalates based on their description as oligomers of face-sharing octahedra is shown in Figure 1.

The ionic sublattice is by no means different from “normal”, purely ionic oxometalates, as strongly supported by density functional theory (DFT) calculations.<sup>3</sup> The  $[\text{MO}_4]^{5-}$  anion behaves as a quasi-molecular entity and shows no significant electronic contribution from the 12 coordinating Cs atoms.  $[\text{A}_{12}\text{MO}_4]$  entities (A = alkali metal) of distorted cuboctahedral shape are very common in the structural chemistry of orthometalates, and all of the geometric details in the anionic part of the suboxometalates are very similar to those of anions in comparable ionic oxometalates (see Figure 2).

The additional cesium atom in  $\text{Cs}_9\text{MO}_4 = [\text{Cs}_8\text{MO}_4] \cdot \text{Cs}$  is coordinated by eight other cesium atoms in the shape of a slightly compressed  $[\text{Cs}_8\text{Cs}]$  cube with Cs–Cs distances between 528.1 and 531.9 pm, reminiscent of the body-centered cubic packing in elemental cesium with comparable Cs–Cs distances of 525 pm.<sup>3,6</sup> It has no direct contact to the oxometalate anion. The likeness of the local surroundings of both the oxometalate anion and the cesium atom in the suboxometalates  $\text{Cs}_9\text{MO}_4$  to those in the ionic structures on the one hand and metallic cesium on the other hand emphasizes the character of an intergrowth structure with two independent sublattices. However, the two sublattices influence each other slightly: The isolated cesium atom shows higher s electron density than  $\text{Cs}^0$  because of the compressed cubic environment and consequently must be addressed as partially negatively charged  $\text{Cs}^{\delta-3}$ .

$\text{Cs}_9\text{MO}_4$  can be formally divided into two sublattices according to  $[\text{Cs}_8\text{MO}_4] \cdot \text{Cs}$ , as can many of the alkali metal suboxides ( $\text{Rb}_6\text{O} = \text{Rb}_9\text{O}_2 \cdot 3\text{Rb}$ ,  $\text{Cs}_8\text{O} = [\text{Cs}_{11}\text{O}_3] \cdot \text{Cs}$ ,  $\text{Cs}_7\text{O} = [\text{Cs}_{11}\text{O}_3] \cdot 10\text{Cs}$ ).<sup>4</sup> Following this analogy, the more cesium-poor suboxometalate  $\text{Cs}_8\text{MO}_4$  can be postulated (paralleling  $\text{Cs}_{11}\text{O}_3$ ) as well as more cesium-rich suboxometalates,  $[\text{Cs}_8\text{MO}_4] \cdot n\text{Cs}$ . The introduced terms “cesium-poor” and “cesium-rich” refer to the Cs:O ratio in the respective empirical formulas. “Cesium-rich” means a high Cs:O ratio, leading to a higher number of metallic cesium atoms in the compound according to the formal division of the sum formulas as above. The comparison of suboxides and suboxometalates with respect to the variable amount of metallic

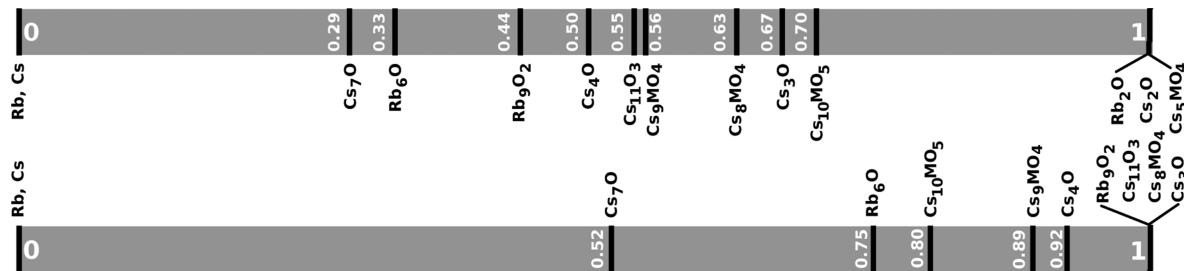


**Figure 3.** Comparison of alkali metal suboxides and suboxometalates with respect to their alkali metal contents. Upper scale: arrangement of the compounds following the mean formal oxidation number of the alkali metal atom (given in white). Lower scale: arrangement following the quotient number of alkali metal atoms per total number of alkali metal atoms in the compound (given in white).

**Table 1. Crystallographic Data and Details on Structure Solution and Refinement of  $\text{Cs}_{10}\text{MO}_5$  in the Orthorhombic and Monoclinic Modifications; Numbers in Parentheses Are Standard Deviations in Units of the Last Digit**

	$\text{Cs}_{10}\text{AlO}_5$	$\text{Cs}_{10}\text{Al}_{0.15}\text{Fe}_{0.85}\text{O}_5$	$\text{Cs}_{10}\text{Al}_{0.32}\text{Ga}_{0.68}\text{O}_5$	$\text{Cs}_{10}\text{AlO}_5$	$\text{Cs}_{10}\text{GaO}_5$
crystal system		orthorhombic		monoclinic	
space group		$Pnmm$ (No. 58)		$C2/c$ (No. 15)	
lattice parameters/ $\text{\AA}$ , deg	$a = 11.158(3)$ $b = 23.693(15)$ $c = 12.229(3)$	$a = 11.227(2)$ $b = 23.742(9)$ $c = 12.371(2)$	$a = 11.1799(2)$ $b = 23.6590(5)$ $c = 12.2957(2)$	$a = 21.195(12)$ $b = 12.480(4)$ $c = 24.12(3)$ $\beta = 98.06(12)$	$a = 21.3877(17)$ $b = 12.4608(11)$ $c = 24.064(2)$ $\beta = 98.558(6)$
volume/ $10^6 \text{\AA}^3$	3233(2)	3297.5(15)	3252.28(10)	6318(9)	6341.8(9)
$Z$	4	4	4	8	8
measured density/ $\text{g}\cdot\text{cm}^{-3}$	2.950	2.943	2.992	3.020	3.076
diffractometer		STOE IPDS-I, Mo $\text{K}\alpha$ radiation, graphite monochromator, room temperature			
absorption coefficient/ $\text{mm}^{-1}$	11.159	11.281	11.628	11.421	12.181
$\theta$ -range/deg	1.87–20.00	2.45–25.00	1.72–25.00	2.02–25.62	1.90–25.00
index ranges	$-10 \leq h \leq 10$ $-22 \leq k \leq 22$ $-11 \leq l \leq 11$	$-13 \leq h \leq 13$ $-28 \leq k \leq 28$ $-13 \leq l \leq 14$	$-13 \leq h \leq 13$ $28 \leq k \leq 28$ $-14 \leq l \leq 14$	$-25 \leq h \leq 25$ $-15 \leq k \leq 15$ $-29 \leq l \leq 29$	$-25 \leq h \leq 24$ $-14 \leq k \leq 14$ $-28 \leq l \leq 28$
no. of measured reflns	10666	17337	34069	25888	27001
no. of independent reflns	1583	3025	3014	5903	5443
no. of independent reflns with $I \geq 2\sigma(I)$	831	1041	2429	2097	2636
$R_{\text{int}}$	0.1139	0.1707	0.0697	0.1899	0.2020
$R_{\sigma}$	0.1037	0.1389	0.0246	0.1704	0.1321
$F(000)$	2412	2457	2461	4824	4968
corrections		Lorentz, polarization, absorption			
absorption correction		semiempirical		numerical	
structure solution			direct methods <sup>13</sup>		
structure refinement			full-matrix least-squares on $F^2$ <sup>13</sup>		
no. of least-squares parameters	84	86	85	146	146
GOF on $F^2$	0.693	0.743	1.280	0.790	1.132
$R$ values (for reflns with $I \geq 2\sigma(I)$ )	$R_1 = 0.0316$ $wR_2 = 0.0562$	$R_1 = 0.0556$ $wR_2 = 0.1325$	$R_1 = 0.0423$ $wR_2 = 0.1540$	$R_1 = 0.0783$ $wR_2 = 0.1667$	$R_1 = 0.1273$ $wR_2 = 0.3252$
$R$ values (all data)	$R_1 = 0.0751$ $wR_2 = 0.0603$	$R_1 = 0.1495$ $wR_2 = 0.1537$	$R_1 = 0.0616$ $wR_2 = 0.1715$	$R_1 = 0.1854$ $wR_2 = 0.1899$	$R_1 = 0.2414$ $wR_2 = 0.3730$
residual electron density/ $\text{e}\cdot 10^{-6} \text{ pm}^{-3}$	0.587/−0.734	1.366/−0.884	1.164/−1.619	1.129/−1.263	2.460/−2.156

alkali metal is given in Figure 3. The upper scale emphasizes the overall electron count in the respective phases, and the lower scale emphasizes structural similarities between them.

Following the similarities between the building principles of alkali metal suboxides and subnitrides on the one hand and cesium suboxometalates on the other hand, we found it worthwhile to extend the structural plethora of suboxides by preparing new suboxometalates with both higher and lower cesium contents than  $\text{Cs}_9\text{MO}_4$ . We have synthesized and characterized a family of new cesium-poor suboxometalates with composition  $\text{Cs}_{10}\text{MO}_5$  ( $\text{M} = \text{Al}, \text{Ga}, \text{Fe}$ ). Here we show that

their crystal structures indeed follow the above-mentioned structural building principles but at the same time broaden the spectrum of compounds of the suboxometalates by unexpected novel combinations of known building units.

## EXPERIMENTAL SECTION

**Materials.** As starting materials, the commercially available oxides  $\text{Al}_2\text{O}_3$  (Alfa Aesar, 99.99%),  $\text{Fe}_2\text{O}_3$  (Merck, 99%), and  $\text{Ga}_2\text{O}_3$  (Sigma-Aldrich, 99.99%) were employed and dried under dynamic vacuum at 300–400 °C prior to use.

$\text{Cs}_2\text{O}$  was prepared following a modified version of the pathway reported by Brauer.<sup>8</sup> About 10 g of cesium metal was reacted with a

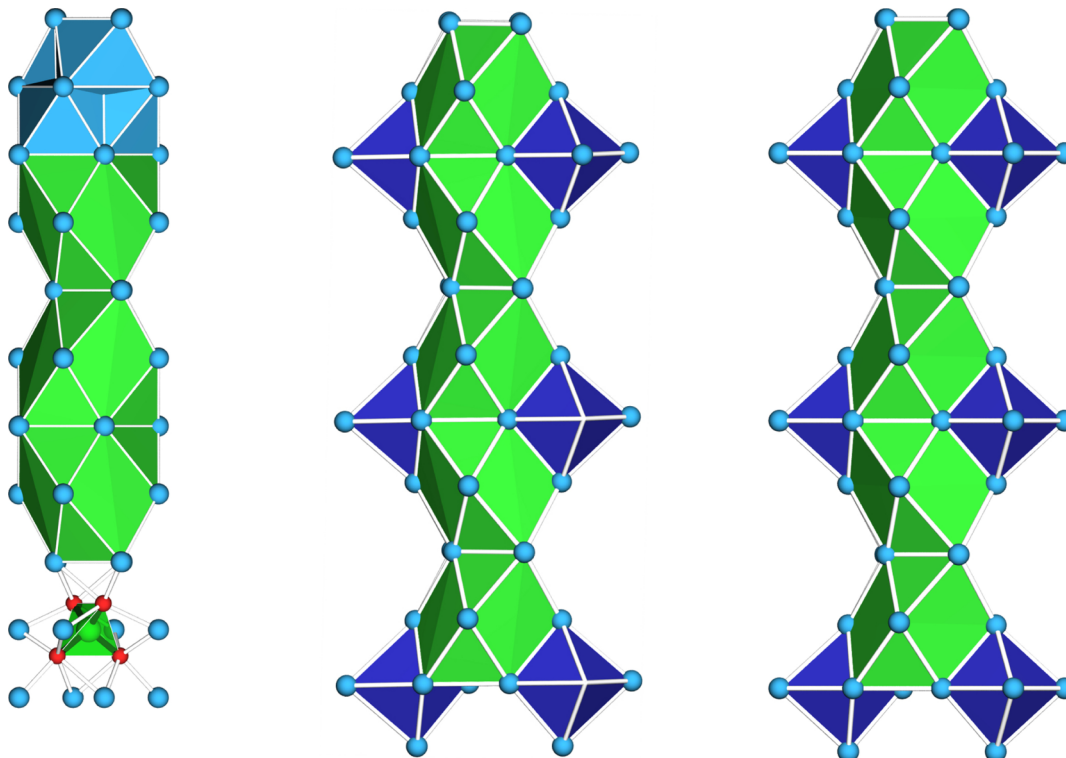


**Figure 4.** Comparison of the columnar building units in (left)  $\text{Cs}_9\text{AlO}_4$ , (center)  $\text{Cs}_{10}\text{AlO}_5$  monoclinic modification, and (right)  $\text{Cs}_{10}\text{AlO}_5$  orthorhombic modification. On the left, three ways of presentation as used in Figures 1 and 2 have been combined for clarification. The topological equivalency of the two columns in the two modifications of  $\text{Cs}_{10}\text{AlO}_5$  and their close relation to the column in  $\text{Cs}_9\text{AlO}_4$  is obvious. The blue octahedra are centered with oxide anions and the green distorted cuboctahedra with oxoaluminate anions  $[\text{AlO}_4]^{5-}$ . Cs, blue; Al, green; O, red.

stoichiometric amount of oxygen calculated for  $\text{Cs}_3\text{O}$  under vigorous stirring with initial cooling and then heating of the reaction vessel. The oxygen was generated by thermal decomposition of  $\text{HgO}$  at  $600\text{ }^\circ\text{C}$ .<sup>9</sup> At the end of the reaction, a black compound,  $\text{Cs}_3\text{O}$ , was formed. The reaction progress could be easily monitored by observing the melting point of the reaction product via the binary phase diagram of  $\text{Cs}-\text{O}$ . Subsequently, the reaction mixture was heated to  $160\text{ }^\circ\text{C}$  under vacuum to remove excess cesium by distillation, resulting in the formation of  $\text{Cs}_2\text{O}$ . The purity was controlled by powder X-ray diffraction (see the Supporting Information).

The suboxometalates  $\text{Cs}_{10}\text{MO}_5$  were synthesized from mixtures of  $\text{Cs}$ ,  $\text{M}_2\text{O}_3$ , and  $\text{Cs}_2\text{O}$  in the ratio 6:1:7. All operations were performed under an argon atmosphere. The reaction mixture was weighed in a tantalum crucible cleaned priorly with a mixture of concentrated  $\text{H}_2\text{SO}_4$ ,  $\text{HNO}_3$ , and HF. To prevent distillation of cesium, the crucibles were placed in steel autoclaves positioned in quartz tubes under argon and placed in a tube furnace. The samples were heated to  $250\text{--}320\text{ }^\circ\text{C}$  for 5 h and then rapidly cooled to room temperature by turning off the furnace. Crystals of the suboxometalates  $\text{Cs}_{10}\text{MO}_5$  were always accompanied by the cesium-rich suboxometalates  $\text{Cs}_9\text{MO}_4$  and liquid cesium suboxide mixtures.

**X-ray Diffraction Analysis.** Single crystals were selected under dry paraffin oil with the aid of a stereo microscope and sealed in glass capillaries filled with dry paraffin oil. Single-crystal X-ray data were collected at room temperature on an IPDS-1 single-crystal diffractometer (STOE & Cie. GmbH, Darmstadt, Germany) equipped with an imaging plate detector and graphite-monochromatized  $\text{Mo K}\alpha$  or  $\text{Ag K}\alpha$  radiation. Absorption corrections were performed by numerical methods on the basis of indexed crystal faces or by semiempirical methods on the basis of data redundancy.<sup>10–12</sup> Structure solution was carried out with direct methods<sup>13</sup> and structure refinement with least-squares methods.<sup>13</sup>

Excess liquid cesium suboxide required the samples to be mixed with dried diamond powder for use in powder X-ray diffraction experiments. The samples were sealed in glass capillaries. Measurements were

executed at  $298\text{ K}$  on a Stadi P system (STOE & Cie. GmbH, Darmstadt, Germany) with  $\text{Mo K}\alpha$  radiation and the para-focusing Debye–Scherrer geometry ( $\text{Ge}(111)$  monochromator,  $\text{Si}$  as an external standard). For data handling and processing, the implemented software WINXPOW was employed,<sup>14</sup> and for Rietveld refinement, the software TOPAS was applied.<sup>15</sup>

Details on data collection, lattice parameters, and structure refinement are compiled in Table 1, while fractional atomic coordinates, isotropic thermal displacement parameters, anisotropic thermal displacement parameters, and relevant interatomic distances and angles are compiled in the Supporting Information. Further information on data collection and structural details can be obtained by requesting the respective crystal information files (CIFs) from Fachinformationszentrum Karlsruhe, D-76344 Eggenstein-Leopoldshafen, Germany (e-mail: crysdata@fiz-karlsruhe.de) upon quoting the depository numbers CSD-429344 ( $\text{Cs}_{10}\text{AlO}_5$ , monoclinic modification), CSD-429345 ( $\text{Cs}_{10}\text{AlO}_5$ , orthorhombic modification), CSD-429355 ( $\text{Cs}_{10}\text{GaO}_5$ ), CSD-429356 ( $\text{Cs}_{10}(\text{Al}/\text{Ga})\text{O}_5$ ), and CSD-429358 ( $\text{Cs}_{10}(\text{Al}/\text{Fe})\text{O}_5$ ), the names of the authors, and the citation of the paper.

**Differential Thermal Analysis.** Differential thermal analysis was performed with a differential calorimeter (self-constructed, Max-Planck-Institut für Festkörperforschung, Stuttgart, Germany). Measurements were conducted in sealed tantalum crucibles. The heating rate was  $3\text{ K}\cdot\text{min}^{-1}$ , and the cooling rate was  $1\text{ K}\cdot\text{min}^{-1}$ . Potassium nitrate was used as a reference (phase transformation at  $401\text{ K}$ , melting point at  $610\text{ K}$ ). Data were exported with the device-specific software and evaluated with ORIGIN.<sup>16</sup>

**Density Functional Theory Calculations.** DFT calculations on the relative stabilities of the two modifications of  $\text{Cs}_{10}\text{AlO}_5$  were performed with VASP using the generalized gradient approximation (GGA) and the Perdew–Burke–Ernzerhof (PBE) functional with 500 eV and PW cutoff. For the orthorhombic and monoclinic modifications,  $2 \times 1 \times 2$  and  $1 \times 2 \times 1$  matrixes were applied, respectively.

**Table 2.** Apical Cs–Cs Distances [pm] in  $[Cs_6O]$  Octahedra from Cesium Suboxides and Cesium Oxide and Averaged Values in Comparison with the Empty Voids in Suboxometalates  $Cs_9MO_4$  and the Unoccupied Interstices d1, d2, and d3 and Occupied Interstices (d4, bold numbers) in the Suboxometalates  $Cs_{10}MO_5$  ( $\varnothing$  Indicates the Arithmetic Average)

$Cs_7O^4$	$Cs_4O^4$	$Cs_{11}O_3^{17}$	$Cs_3O^{18}$	$Cs_2O^{19}$	
563.4 (3x)	564.4 (3x)	566.6 (1x)	578.0 (3x)	572.5 (3x)	
565.8 (6x)	566.2 (6x)	568.6 (1x)			
		562.4 (1x)			
		570.6 (1x)			
		572.9 (1x)			
		558.5 (1x)			
		572.0 (1x)			
		570.9 (1x)			
		569.4 (1x)			
$\varnothing_{Cs_7O} = 565.0$		$\varnothing_{Cs_4O} = 565.6$		$\varnothing_{Cs_{11}O_3} = 568.0$	
		$\varnothing_{Cs_3O} = 578.0$		$\varnothing_{Cs_2O} = 572.5$	
$\varnothing_{\text{overall}} = 567.8$					
$Cs_9AlO_4$	$Cs_9GaO_4$	$Cs_9FeO_4$	$Cs_9ScO_4$	$Cs_9InO_4$	
621.0	624.4	628.7	639.6	645.0	
$\varnothing_{\text{overall}} = 631.7$					
$Cs_{10}AlO_5$ (orthorhombic)	$Cs_{10}AlO_5$ (monoclinic)	$Cs_{10}GaO_5$ (monoclinic)	$Cs_{10}(Al/Ga)O_5$ (orthorhombic)	$Cs_{10}(Al/Fe)O_5$ (orthorhombic)	
d1: 620.6	619.2	627.6	623.5	626.9	
d2: 643.5	644.5	655.7	649.2	655.1	
d3: 602.3	610.7	612.9	606.0	610.2	
<b>d4: 579.4</b>	<b>585.4</b>	<b>584.8</b>	<b>580.4</b>	<b>582.0</b>	
$\varnothing_{d4} = 582.4$					

## RESULTS AND DISCUSSION

The crystal structures of both the cesium-rich suboxometalates  $Cs_9MO_4$  and the cesium-poor suboxometalates  $Cs_{10}MO_5$  with M = Al, Ga, Fe can be constructed by packing of columnar units as shown in Figure 4. Subdividing the crystal structures into smaller building blocks is a common picture in solid-state chemistry, even in cases where these building blocks are merely figurative and do not refer to chemically separated entities that could, e.g., be extracted from the structure by a solvent. In many solid-state structures, the bonding forces between the building units are as strong as the ones within them, and the definition of such subunits is arbitrary and justified only by a better topological understanding of the complete structure. In the alkali metal suboxometalates, however, the columnar subunits can effectively be addressed as chemically independent entities, and the assumption of columnar clusters formed in the respective melts may be applicable.

The  $[Cs_{10}MO_5]$  columns present in the cesium-poor suboxometalates  $Cs_{10}MO_5$  can be derived from the  $[Cs_8MO_4]$  columns in the cesium-rich suboxometalates  $Cs_9MO_4$  by inserting additional  $[Cs_6O]$  octahedra via face sharing. These octahedra show similar features as the ones constituting the various cluster units in the binary alkali metal suboxides. The Cs–O distances range from 565 to 578 pm in the suboxides and from 579 to 585 pm in the suboxometalates (see Table 2 and the Supporting Information). As a result of the strong Coulomb repulsions between the oxide ions centering the  $[Cs_6O]$  octahedra and the adjacent  $[MO_4]^{5-}$  oxometalate anions, the oxide anions are shifted considerably from the centers of the  $[Cs_6O]$  octahedra (see Figure 6, left). The same situation is found in the  $[Cs_{11}O_3]$  triple octahedra in the cesium suboxides.

The comparison of the  $[Cs_8MO_4]$  columns from the suboxometalates  $Cs_9MO_4$  with the  $[Cs_{10}MO_5]$  columns shows that the insertion of  $[Cs_6O]$  units, sharing common faces with only a quarter of all available interstices in the  $[Cs_8MO_4]$  unit, leads to a distortion of the columns and lower symmetry. In the  $[Cs_8MO_4]$  columns, all four topologically suitable positions for the insertion of  $[Cs_6O]$  groups are symmetrically equivalent. The

M atom at the center of the distorted cuboctahedron has point symmetry  $4\bar{2}m$ . In  $Cs_{10}MO_5$ , only one of the possible positions is occupied in both the monoclinic and orthorhombic modifications. The M atoms only have point symmetry 1 (monoclinic structures) or 2 (orthorhombic structures). The distortion of the columns is necessary to account for the preferential apical Cs–Cs distance in a  $[Cs_6O]$  octahedron, which can be derived from a comparison of all binary cesium–oxygen compounds (see Table 2). The undistorted  $[Cs_8MO_4]$  column has longer Cs–Cs distances in the possible positions, so the insertion of a shorter octahedron leads to alternating Cs–Cs distances along the  $[Cs_{10}MO_5]$  column. This geometric criterion provides an explanation of why the variety of M in  $Cs_9MO_4$  is higher (M = Al, Ga, Fe, Sc, or In and mixed crystals thereof) than in  $Cs_{10}MO_5$  (M = Al, Ga, or Fe and mixed crystals thereof). It was shown that the increasing ionic radius of M in going from  $Al^{3+}$  to  $In^{3+}$  influences only the length of the  $[Cs_8MO_4]$  column but not its diameter,<sup>3</sup> and therefore, the distortion of the Cs–Cs distances necessary to accommodate the insertion of a  $[Cs_6O]$  octahedron is smaller and feasible only for smaller M = Al, Ga, or Fe. The interstices are so large in  $Cs_9InO_4$  and  $Cs_9ScO_4$  that the distortion becomes unfavorable (see Figure 5), and no cesium-poor suboxoindate or suboxoscandate is formed. The limit distance in  $Cs_9MO_4$  suboxometalates lies around 630 pm for the apical Cs–Cs distance in the column. Below this value, the distortion toward the optimal value of 567.8 pm still is possible. Parallel to the decrease of one of the four distances (d4 in Table 2), an increase in one of the other distances (d2 in Table 2) has to occur, constituting the geometrical limit for the Cs-poor suboxometalates.

The cesium suboxometalates  $Cs_{10}MO_5$  crystallize in two modifications. The representatives of the two crystal structures are strictly isotopic for different M metals. Consequently, mixed crystals  $Cs_{10}Al_xGa_{1-x}O_5$  and  $Cs_{10}Al_xFe_{1-x}O_5$  can be prepared in which no ordering of the different metals occurs. This finding is consistent with the mixed-crystal behavior of the suboxometalates  $Cs_9MO_4$ . In contrast to these, the substitution of cesium by rubidium was never found for the suboxometalates  $Cs_{10}MO_5$ .

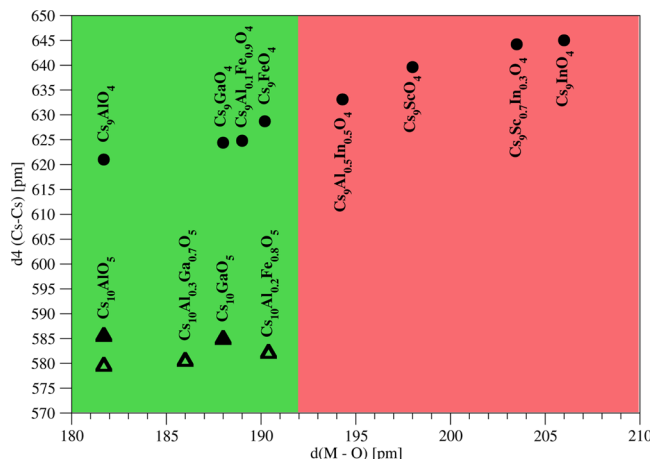


**Figure 5.** Dependence of the apical Cs–Cs distance  $d_4$  (see Table 2) on the size of the  $[MO_4]^{5-}$  anion in suboxometalates. For  $M = Al$ ,  $Ga$ , or  $Fe$ , the distances are suitable for insertion of  $[Cs_6O]$ , while for  $M = Sc$  or  $In$  the distances are too large. Circles, suboxometalates  $Cs_9MO_4$ ; open triangles, suboxometalates  $Cs_{10}MO_5$  (orthorhombic modification); solid triangles, suboxometalates  $Cs_{10}MO_5$  (monoclinic modification).

This can be understood because in  $Cs_{9-x}Rb_xMO_4$ , only the purely metallic Cs position is substituted, whereas in  $Cs_{10}MO_5$  no such purely metallic position is present.

The crystal structures of the two modifications are shown in Figure 6. Both modifications are built from the same columnlike motifs with composition  $[Cs_{10}MO_5]$ , built from  $[Cs_8MO_4]$  columns as found in the cesium-rich suboxometalates  $Cs_9MO_4$ , but with additional  $[Cs_6O]$  octahedra condensed via common faces (see Figure 4). Arranging the  $[Cs_{10}MO_5]$  columns differently leads to the two modifications: either a parallel arrangement (orthorhombic modification) or a skew arrangement (monoclinic modification).

Comparison of the two modifications shows high similarity in geometric details of the  $[Cs_{10}MO_5]$  columns (see the Supporting Information) and, as a consequence, similar unit cell volumes. For example, the orthorhombic modification of  $Cs_{10}AlO_5$  has a unit cell volume of  $3233(3)$  Å $^3$  and  $Z = 4$ , whereas its monoclinic modification has a unit cell volume of  $6318(9)$  Å $^3$  and  $Z = 8$ . The orthorhombic modification thus has a volume per formula unit that is about 2% higher than that of the monoclinic modification, and the density of the orthorhombic modification ( $2.950$  g·

cm $^{-3}$ ) is slightly lower than that of the monoclinic modification ( $3.020$  g·cm $^{-3}$ ). Because of these very small differences, it can be estimated that the difference in the thermodynamic stabilities of the two modifications also is only marginal. In our experiments it remained unclear which parameter determines whether the orthorhombic or the monoclinic modification can be obtained; however, it was normally observed that in a given sample, single-crystal specimens belonged to only one of the two modifications.

Thermoanalytic investigations show the difficulty in deliberately synthesizing one of the two modifications of the new suboxometalates as a phase-pure sample. A 7:6:1 mixture of cesium oxide, cesium metal, and  $Al_2O_3$ , fitting for the synthesis of  $Cs_{10}AlO_5$ , was heated to  $400$  °C, cooled to room temperature, and again heated to  $400$  °C and cooled to room temperature (see Figure 7). The first heating curve of the pristine reaction mixture

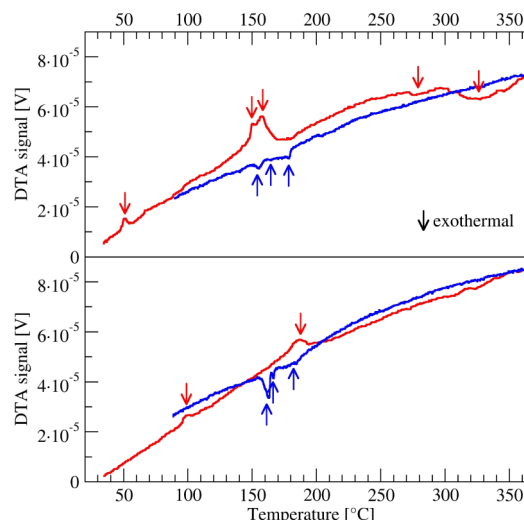


**Figure 7.** Differential thermal analysis of reaction mixtures for  $Cs_{10}AlO_5$ : (top) heating and cooling curves for a pristine 7:6:1 mixture of  $Cs_2O$ ,  $Cs$ , and  $Al_2O_3$ ; (bottom) second heating and cooling curves for the same sample.

shows three endothermal and two weak and broad exothermal signals. At about  $50$  °C, a cesium-rich suboxidic component spontaneously formed from Cs and  $Cs_2O$  melts, in accordance with the Cs–O phase diagram.<sup>17</sup> At ca.  $150$  °C, two adjacent signals show further melting processes of more oxygen-rich

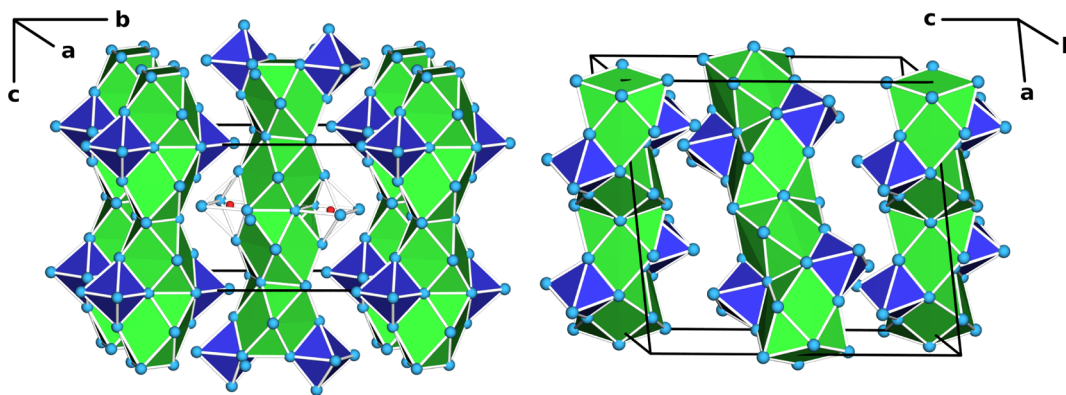


**Figure 6.** Crystal structures of the two modifications of  $Cs_{10}MO_5$ : (left) orthorhombic modification, space group  $Pnnm$ ; (right) monoclinic modification, space group  $C2/c$ . In the left picture, two  $[Cs_6O]$  octahedra are drawn transparent to show the shift of the oxide anions from the center of the octahedron. Cs atoms, blue; M atoms, surrounded by green polyhedra; O atoms, red.

suboxidic species. At ca. 270 and 320 °C two exothermal reactions occur, one belonging to the formation of  $\text{Cs}_9\text{AlO}_4$  and the other to the formation of  $\text{Cs}_{10}\text{AlO}_5$ . As slow cooling of reaction mixtures from 350 °C always yields phase-pure samples of  $\text{Cs}_9\text{AlO}_4$  and rapid cooling yields mixtures of  $\text{Cs}_9\text{AlO}_4$  and  $\text{Cs}_{10}\text{AlO}_5$  (see the Supporting Information), the higher reaction signal belongs to the formation of  $\text{Cs}_9\text{AlO}_4$  by consumption of  $\text{Cs}_{10}\text{AlO}_5$ . The cooling curve shows two signals at ca. 155 and 160 °C belonging to the solidification of residual suboxidic species and a third signal at ca. 175 °C belonging to the crystallization of  $\text{Cs}_9\text{AlO}_4$ . The second heating consequently shows no reaction signals and shifted endothermic effects belonging to the melting of the suboxide species, as the composition of the reaction mixture has been shifted toward more cesium-poor suboxides by the formation of  $\text{Cs}_9\text{AlO}_4$ . The effects of the first cooling process can be reproduced in the second cooling. It seems clear that the formation of  $\text{Cs}_9\text{AlO}_4$  renders the phase-pure synthesis of either modification of  $\text{Cs}_{10}\text{AlO}_5$  difficult. The formation of the more cesium-poor suboxometalate and its decomposition to the more cesium-rich suboxometalate plus cesium suboxides occur at very closely neighboring temperatures.

DFT calculations on the basis of the single-crystal structure models showed that the electronic contributions of the two modifications differed only by 1.1  $\text{kJ}\cdot\text{mol}^{-1}$ , with the orthorhombic modification being slightly thermodynamically preferred. However, the calculations of the relative energies are based on the electronic structures only. Following a concept based on information theory, the respective complexities of the two modifications can be quantified.<sup>20</sup> The difference is again very small, with 256 bits for the orthorhombic modification and 224 bits for the monoclinic modification. Consistent with the calculations, the Ostwald rule of stages<sup>21</sup> predicts the orthorhombic modification to be the thermodynamically stable one at room temperature because of the higher complexity.

## ■ CONCLUSION

The structural chemistry of cesium suboxometalates shows the chance to twin ionic and metallic substructures in ordered crystals. This leads to the mixing of typical physical properties common to both systems. Future work may show the extent to which this route leads to systems with interesting combinations such as, e.g., high electric and low thermal conductivity, multiferroic properties, further reduction of the metallic sublattice toward ordered quantum dots, and others. At the moment, this chemistry is constrained to alkali-metal-rich systems showing high reactivity toward ambient conditions. However, combinations containing even larger anionic sublattices such as Keggin ions and polyoxometalates combined with substitution of the highly reactive alkali metals by other metals can help to find ways toward more stable compounds suitable for application purposes.

## ■ ASSOCIATED CONTENT

### S Supporting Information

Tables of fractional atomic coordinates, coefficients of the anisotropic displacement parameters, and selected interatomic distances and angles of all discussed compounds; Rietveld refinement data and plot for the educt  $\text{Cs}_2\text{O}$  and the product  $\text{Cs}_{10}\text{AlO}_5$  (orthorhombic) with respective side phases. The Supporting Information is available free of charge on the ACS Publications website at DOI: 10.1021/acs.inorgchem.Sb01060.

## ■ AUTHOR INFORMATION

### Corresponding Author

\*Phone: +49 (0)89 2180 77421. Fax: +49 (0)89 2180 77440. E-mail: constantin.hoch@cup.lmu.de.

### Notes

The authors declare no competing financial interest.

## ■ ACKNOWLEDGMENTS

The authors thank Kristina Ritter, Jasmin Dums, Patrick Hirschle, Irina Zaytseva, and Claudia Lenk for the sample preparations. Roland Eger at MPI FKF, Stuttgart, Germany, is gratefully acknowledged for help in the thermoanalytic investigations. The DFT calculations kindly were provided by Prof. Dr. R. Dronskowski and his group at RWTH Aachen, Germany.

## ■ REFERENCES

- (1) Gunnarsson, O.; Calandra, M.; Han, J. E. *Rev. Mod. Phys.* **2003**, *75*, 1085–1099.
- (2) (a) Hoch, C.; Simon, A. *Angew. Chem.* **2012**, *124*, 3316–3319; (b) Hoch, C.; Simon, A. *Angew. Chem., Int. Ed.* **2012**, *51*, 3262–3265; (c) Tambornino, F.; Hoch, C. *J. Alloys Compd.* **2015**, *618*, 299–304; (d) Tambornino, F.; Hoch, C. *Z. Anorg. Allg. Chem.* **2015**, *641*, 537–542.
- (3) (a) Hoch, C.; Bender, J.; Simon, A. *Angew. Chem.* **2009**, *121*, 2451–2453; (b) Hoch, C.; Bender, J.; Simon, A. *Angew. Chem., Int. Ed.* **2009**, *48*, 2415–2417; (c) Hoch, C.; Bender, J.; Wohlfahrt, A.; Simon, A. Z. *Anorg. Allg. Chem.* **2009**, *635*, 1777–1782; (d) Hoch, C.; Simon, A.; Lee, C.; Whangbo, M. H.; Köhler, J. Z. *Kristallogr.* **2011**, *226*, 553–556; (e) Hoch, C. *Z. Naturforsch.* **2011**, *66b*, 1248–1254.
- (4) (a) Simon, A.; Deiseroth, H. J. *Rev. Chim. Miner.* **1976**, *13*, 98–112; (b) Simon, A.; Deiseroth, H. J.; Westerbeck, E.; Hillenkötter, B. Z. *Anorg. Allg. Chem.* **1976**, *423*, 203–211; (c) Simon, A. Z. *Anorg. Allg. Chem.* **1976**, *422*, 208–218.
- (5) (a) Rauch, P. E.; Simon, A. *Angew. Chem.* **1992**, *104*, 1505–1506; (b) Rauch, P. E.; Simon, A. *Angew. Chem., Int. Ed. Engl.* **1992**, *31*, 1519–1521; (c) Snyder, G. F.; Simon, A. *Angew. Chem.* **1994**, *106*, 713–715; (d) Snyder, G. F.; Simon, A. *Angew. Chem., Int. Ed. Engl.* **1994**, *33*, 689–691; (c) Snyder, G. J.; Simon, A. *J. Am. Chem. Soc.* **1995**, *117*, 1996–1999.
- (6) Barrett, C. S. *Acta Crystallogr.* **1956**, *9*, 671–677.
- (7) Bender, J.; Wohlfarth, A.; Hoch, C. *Z. Naturforsch.* **2010**, *65b*, 1416–1426.
- (8) Brauer, G. *Handbuch der Präparativen Anorganischen Chemie*, 2nd ed.; Ferdinand Enke Verlag: Stuttgart, Germany, 1962; Vol. 1, p 978.
- (9) Simon, A. Z. *Anorg. Allg. Chem.* **1973**, *395*, 301–319.
- (10) X-Area, version 1.39; Stoe & Cie.: Darmstadt, Germany, 2006.
- (11) X-Shape, version 2.07; Stoe & Cie.: Darmstadt, Germany, 2005.
- (12) X-Red, version 1.31; Stoe & Cie.: Darmstadt, Germany, 2005.
- (13) Sheldrick, G. M. *Acta Crystallogr.* **2008**, *A64*, 112–122.
- (14) Winxpow, version 2.09; Stoe & Cie.: Darmstadt, Germany, 2005.
- (15) Coelho, A. A.; Evans, J.; Evans, I.; Kern, A.; Parsons, S. *Powder Diff.* **2011**, *26*, 22–25.
- (16) Origin, version 6.1; OriginLab: Northampton, MA, 1991–2000.
- (17) Simon, A.; Westerbeck, E. Z. *Anorg. Allg. Chem.* **1977**, *428*, 187–198.
- (18) Tsai, K. R.; Harris, P. M.; Lassettre, E. N. *J. Phys. Chem.* **1956**, *60*, 345–347.
- (19) Helms, A.; Klemm, W. Z. *Anorg. Allg. Chem.* **1939**, *242*, 33–40.
- (20) Krivovichev, S. *Acta Crystallogr.* **2012**, *A68*, 393–398.
- (21) Ostwald, W. Z. *Phys. Chem.* **1897**, *22*, 289–330.